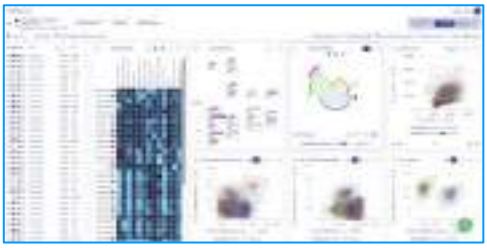
Mitigating the Trade-Off Between Speed and Precision with METAflow™ Software and Attune™ Xenith™ Flow Cytometer in High-Dimensional Cytometry

Introduction

High-dimensional cytometry analysis often requires a compromise between speed and precision. Manual gating is time-consuming, operator-dependent, and difficult to scale, while high-throughput acquisition raises concerns about data quality and reproducibility.

Here, we demonstrate how the combination of Invitrogen™ Attune™ Xenith™ high-speed acquisition and METAflow™ automated, data-driven analysis enables both rapid identification of biologically relevant patterns without compromising results' robustness and reproducibility across users and conditions, even in complex high-dimensional datasets.





Objective

To demonstrate that:

1. Biologically meaningful differences can be identified rapidly without prior assumptions
2. Results are reproducible across acquisition conditions, high acquisition speed does not compromise data quality
3. Complex, high-dimensional datasets can be analyzed in a scalable and standardized workflow, minimizing operator-induced variability
4. This approach can be applied to complex immune profiling panels without losing biological interpretability.

Methods

Specimens: Bone marrow and spleen (multiple files acquired at varying flow rates)

Analysis workflow, leveraging unsupervised tools:

- Data-driven clustering using all markers
- Global exploration of data structure without manual gating
- Lineage-based refinement (T cells, B cells, myeloid/DC/NK) through recursive clustering compartment analysis
- Evaluation across acquisition speeds (200 µL/min vs 1,000 µL/min)
- Comparison with manual gating (4 independent users)

Rapid Identification of Biological Structure

Without preprocessing, prior gating or user assumptions, data-driven clustering followed by global unsupervised analysis reveals clear separation between spleen and bone marrow samples, reflecting their distinct cellular composition. Dimensionality reduction (t-SNE) to visualize global structure of the specimens enables immediate identification of key biological drivers:

- **B220 (B-cell marker)** expression colocalizes with clusters enriched in spleen-derived samples,
- **Ly6C (Myeloid marker)** colocalize with clusters enriched in bone marrow-derived samples.

This initial analysis demonstrates that METAflow can reduce the complexity of a 37-color panel into an interpretable biological structure without requiring manual pre-gating or any preliminary pre-processing, unveiling biological differences in a few clicks.

Key message: Relevant biological structure can be rapidly and consistently identified directly from high-dimensional data without manual intervention.

A. Bone Marrow (top) and Spleen (bottom)

B. Unsupervised clustering (all markers)

C. Lineages identification

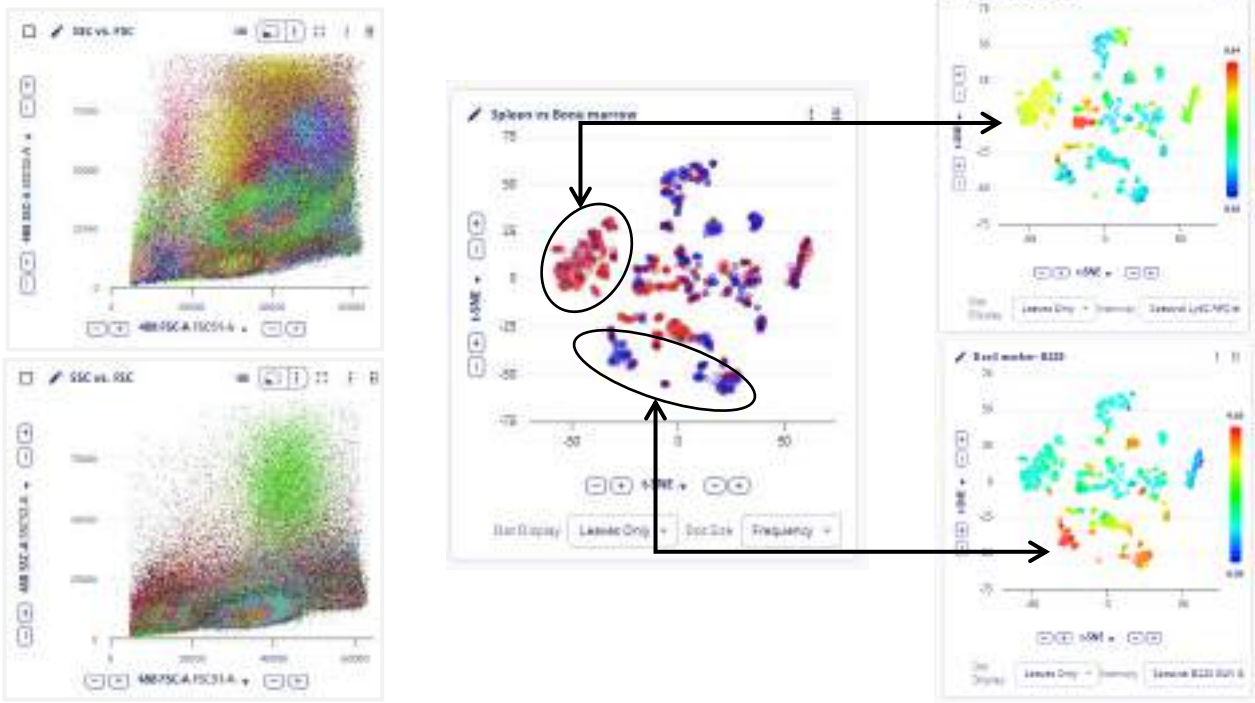


Figure 1. Data-driven clustering reveals global biological differences between spleen and bone marrow. Unsupervised clustering was performed on all files individually, without requiring any prior pre-processing, to exploit all information present in the data set and avoid any bias. **A.** Dot plots show the complexity and distinctiveness of biological specimens in terms of morphology and cellular composition diversity, as reflected by the colors of the clusters (upper plot: spleen ; lower plot: bone marrow). **B.** T-distributed Stochastic Neighbor Embedding (t-SNE) visualization illustrates separation of samples from spleen (blue) and bone marrow (red) based on their underlying cellular composition, independent of acquisition conditions. **C.** Marker expression mapped onto the same t-SNE space highlights key lineage-specific signatures driving this separation. Color gradients represent relative marker expression intensity from low (blue) to high (red).

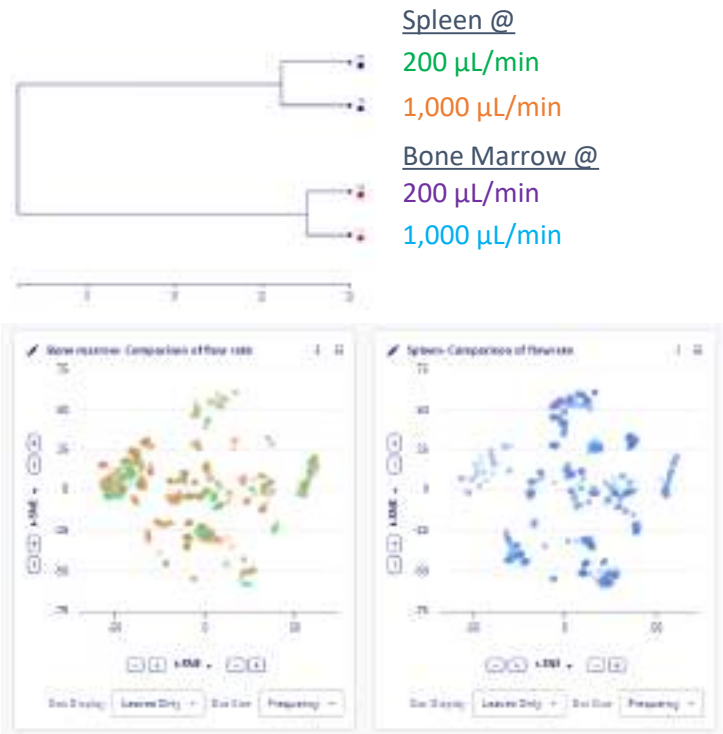
Robustness across acquisition conditions

Samples acquired at 200 µL/min and 1,000 µL/min show overlapping clusters within the UMAP dimensionality reduction space, which preserves both local & global structure, indicating no impact of acquisition speed on data structure. Lineage-specific analyses confirm that population frequencies remain stable across flow rates for a given specimen (bone marrow versus spleen), and biological differences between tissues are preserved across acquisition speeds. Consistent with biological expectations, spleen samples contain a higher proportion of lymphocytes, whereas bone marrow is enriched for myeloid populations. This indicates that increasing acquisition speed does not introduce detectable technical bias in clustering or population quantification.

From an analysis point of view no manual supervised pre-processing is required before comparing populations across files. The METAflow algorithm suite copes automatically with any batch effect or artefact during computing.

Key message: The data-driven, unsupervised clustering engine of METAflow reinforces that global and local data structure is not affected by acquisition speed, demonstrating the robustness of Attune Xenith Cytometer at high-throughput acquisition. Data quality and biological interpretation are maintained.

A. Clustering Is consistent across acquisition speed



B. Population frequency among CD45+ cells



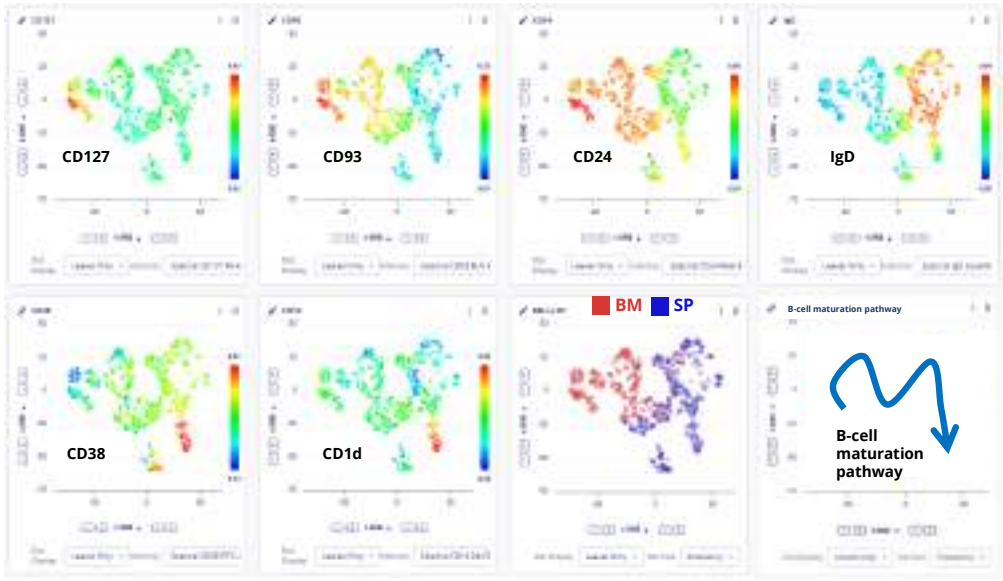
Figure 2. Robustness of clustering and population quantification across acquisition speeds. A. Dendogram illustrates grouping of samples and t-SNE representation from unsupervised clustering of bone marrow (left) and spleen (right) samples acquired at 200 µL/min and 1,000 µL/min. Clusters from both acquisition speeds overlap within each tissue, indicating that acquisition rate does not impact the underlying data structure or clustering performance. **B.** Quantification of major immune compartments (T cells, B cells, and myeloid/DC/NK populations) across tissues and acquisition speeds. Clustering was performed with basic lineage markers without any pre-processing followed by meta-analysis. Population frequencies remain consistent between 200 µL/min and 1,000 µL/min for both spleen and bone marrow (BM) samples.

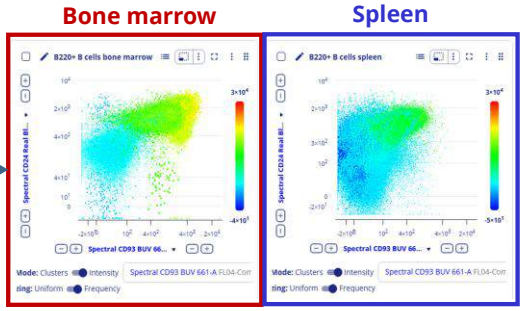
Focused refinement reveals compartment-specific biology

Following identification of B cells as major contributors to tissue separation, clustering enables high-resolution characterization of biologically relevant cell states within this compartment.

As expected, B cell populations exhibit clear tissue-specific differences: early maturation markers such as CD93, CD24, and CD127 are highly expressed in bone marrow, while late markers (CD38, CD1d) are expressed by clusters in spleen samples only; transitional B cell populations are found across both tissues.

A. t-SNE plots illustrating B-cell maturation marker





B. CD93 expression illustrates variation in early B-cell maturation states across tissues.

⬆ CD93 → immature / transitional B cells

⬇ CD93 → mature B cells

Key message. High-dimensional analysis enables resolution of tissue-specific B cell maturation states, demonstrating the ability of METAflow to uncover subtle but biologically relevant differences within complex cell populations.

Figure 3. Tissue-specific B cell compartment signatures revealed by hierarchical analysis. Clustering was applied to the B cell population from bone marrow and spleen samples. **A.** t-SNE of B cell clusters shows clear separation between bone marrow (red) and spleen (blue), reflecting tissue-specific organization of the B cell compartment. Marker expression mapped onto the same t-SNE space highlights differential expressions of CD93, CD24, and CD127, revealing distinct phenotypic gradients across tissues. Color scale indicates relative expression levels from low (blue) to high (red). Each dot represents a cluster, with dot size proportional to cluster frequency. **B.** Dot plots of B220^{+} B cells from bone marrow and spleen, colored by CD93 expression, illustrate differences in variation in early B-cell maturation states across tissues. Bone marrow shows higher CD93 expression consistent with enrichment of immature and transitional-like B-cell states.

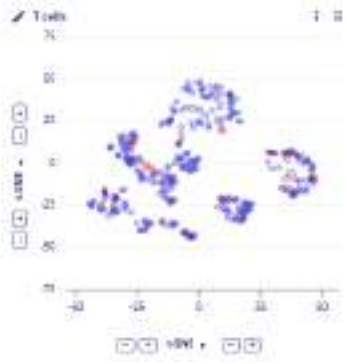
Specificity Control: Preservation of Biological Specificity

Analysis of T cell and myeloid/DC/NK compartments confirms that the workflow preserves biologically meaningful structure without exaggerating weak variation into artificial separation:

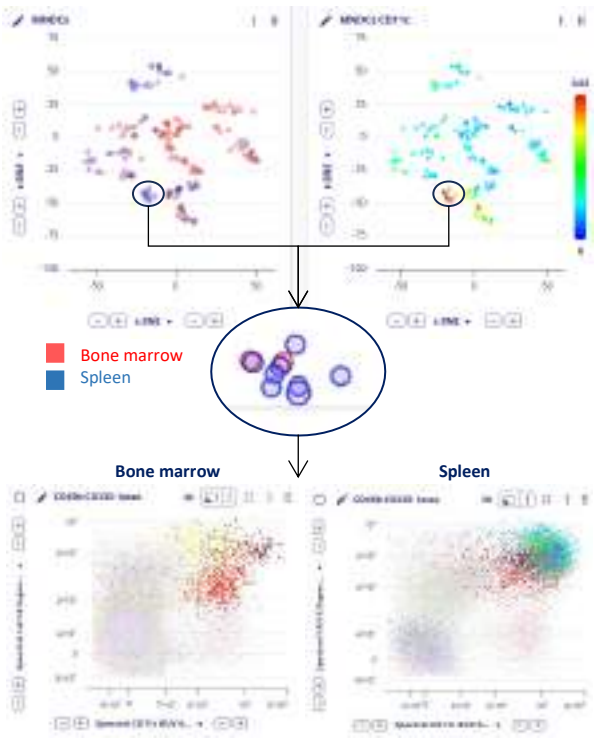
- T-cell populations retain partially overlapping structures despite tissue-dependent differences in abundance.
- The myeloid compartment shows moderate, biologically interpretable variation, with specific dendritic cell populations contributing to observed differences. Marker expression heterogeneity across clusters further supports tissue-specific organization of dendritic cell subsets.

Key message: The workflow preserves biological specificity by capturing true tissue-associated differences without introducing artificial structure, ensuring biologically meaningful interpretation.

A. Minimal variation in T cell populations across tissues



B. Dendritic cell subsets show true tissue-specific differences



C. Increased diversity in DC populations in spleen vs. bone morrow

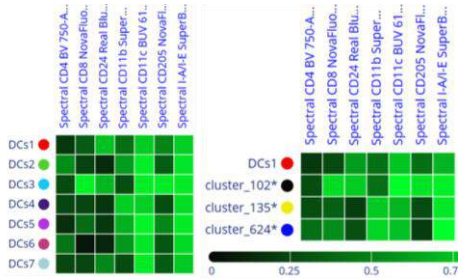


Figure 4. Specificity control: preservation of biological structure without artificial differences. Clustering analysis of T-cell and myeloid/DC/NK (MNDC) compartments from spleen and bone marrow samples demonstrates preservation of biologically meaningful organization without exaggerated artificial separation. **A.** t-SNE representation of T-cell populations shows globally overlapping structure across tissues, consistent with limited global tissue-dependent variation. **B.** t-SNE representation of MNDC populations reveals tissue-associated organization patterns. CD11c expression identifies dendritic cell populations contributing to these differences. Dot plots of CD49b$^-$ CD335$^-$ populations highlight distinct dendritic cell phenotypes between spleen and bone marrow. **C.** Heatmaps of dendritic cell clusters reveal tissue-specific marker expression heterogeneity across DC subsets.

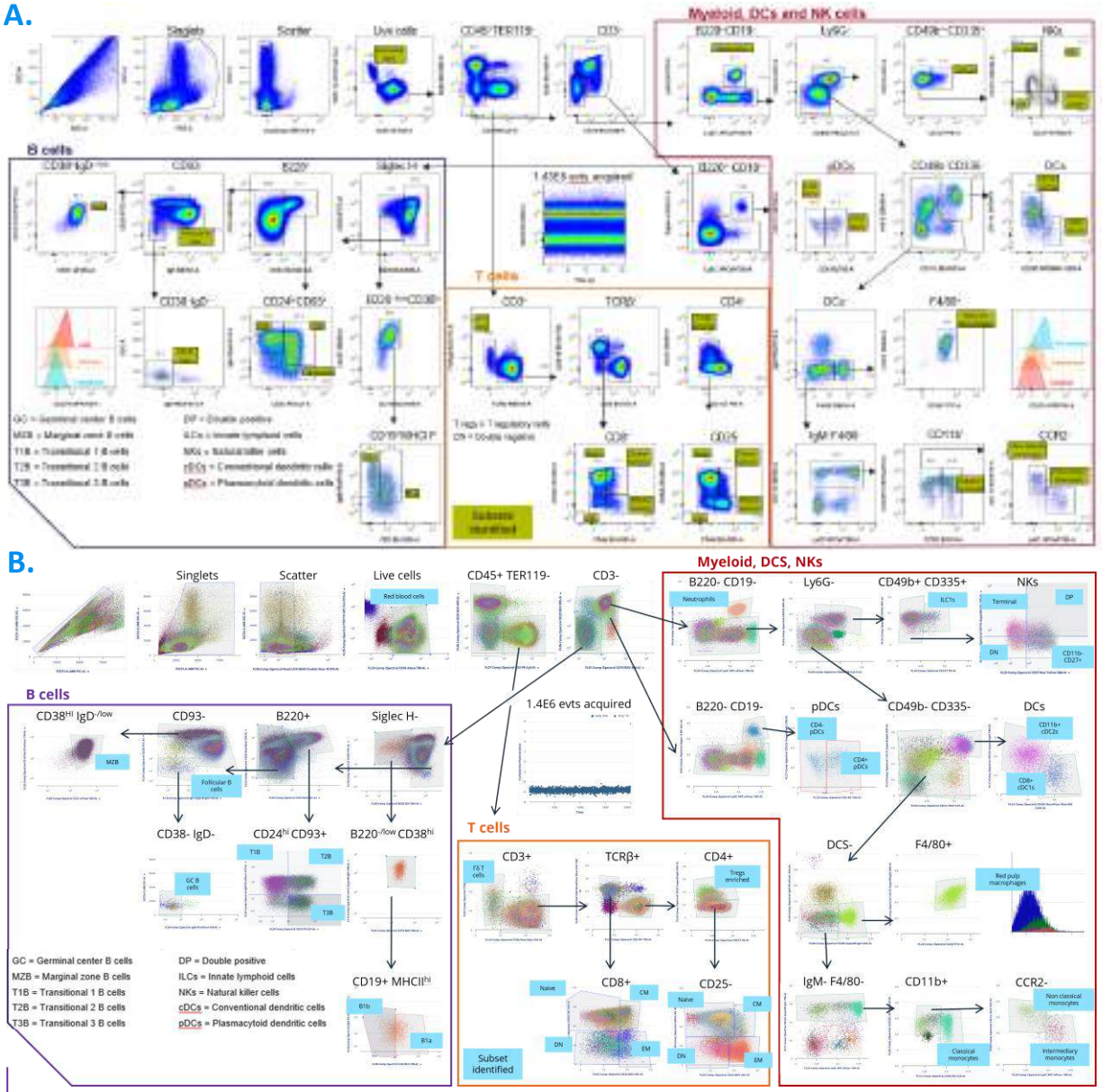


Figure 5. Overview of the full clustering-based analysis, from data cleaning to specific lineages analysis.

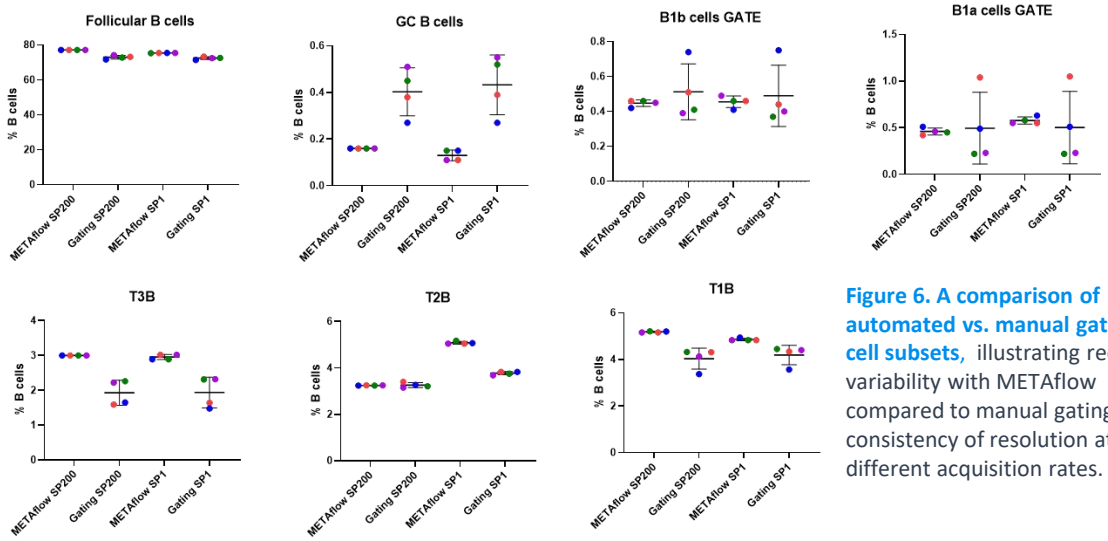


Figure 6. A comparison of automated vs. manual gating of B cell subsets, illustrating reduced variability with METAflow compared to manual gating and consistency of resolution at different acquisition rates.

Figure 5. Overview of the full clustering-based analysis, from data cleaning to specific lineages analysis. A. Manual gating strategy (© Thermo Fisher Scientific). **B.** Semi-supervised analysis combining automated clustering and gating. Every single expected population was identified as cluster(s), as one would expect with manual gating.

Figure 6. Improved reproducibility and reduced operator variability with METAflow compared to manual gating. Following clustering, population frequencies for representative high- and low-abundance B cell populations were compared between METAflow and manual gating across four independent users. Each dot represents the result from a single user. Results are shown for spleen samples at both acquisition speeds (SP200 = 200µL/min, SP1000 = 1000µ/min). High-frequency B cell population (e.g., follicular B cells) shows consistent quantification across all users with both methods. Low-frequency B cell populations (e.g., GC B cells, B1a and B1b cells, T1B, T2B and T3B B cells) exhibit substantial variability with manual gating, while METAflow produces highly consistent results across users.

Validation against manual gating

To evaluate whether automated analysis improves reproducibility, population frequencies were compared between METAflow clustering and conventional manual gating. Population frequencies across high-, medium-, and low-abundance subsets were assessed across four independent users. This comparison directly tests whether the same biological sample produces consistent results when analyzed by different operators. Results show:

- Strong agreement with expert-defined populations,
- Significantly reduced inter-operator variability,
- Consistent results across acquisition speeds.

Across four independent users, full clustering-based analysis with METAflow produced highly consistent population frequencies, whereas manual gating showed greater inter-operator variability, particularly for medium- and low-frequency populations. In addition, the automated workflow reduces analysis time compared to manual gating by automatically adjusting every setting for robust analysis, even across files from distinct tissues showing significant differences, enabling faster generation of reproducible results.

Key message: METAflow standardizes high-dimensional cytometry analysis by reducing user-dependent variability while preserving biologically meaningful differences across tissues and acquisition conditions, even for rare populations detection.

Conclusion

Attune Xenith Cytometer acquisition combined with METAflow analysis enables rapid, scalable, and reproducible interpretation of high-dimensional cytometry data, while preserving biological accuracy. Together, the highly automated workflow reduces dependence on manual pre-processing and gating, and operator-specific interpretation, enabling consistent analysis across users, experiments, and acquisition conditions. Such highly efficient yet robust solutions are gateways for streamlined discoveries.

Explore more services at **thermofisher.com/attunexenith**
Discover METAflow at **metafora-biosystems.com/metaflow** or contact **info@metaflow.bio**

For Research Use Only. Not For Use In Diagnostic Procedures. © 2026 Thermo Fisher Scientific Inc. and Metafora Biosystems. All rights reserved. Attune and Xenith are Trademarks of Thermo Fisher Scientific, Inc. METAflow is a Trademark of Metafora Biosystems.